



# D2.2 Functionalised platform materials by galvanic replacement

Project Information	
Title	From solar energy to fuel: A holistic artificial photosynthesis platform for the production of viable solar fuels
Acronym	REFINE
Project Call	HORIZON-CL5-2022-D3-03
Project Topic	HORIZON-CL5-2022-D3-03-03
Grant Agreement ID	101122323
Project Duration	48 months: 1st November 2023 – 31st October 2027

Document Information	
Contractual Date of Delivery	M18
Actual Date of Delivery	M18
Author(s)	Dragos Neagu, Ubong Essien, Adaora Ekperechukwu, Micah Soriano, Kimia Jafari, Alexander Sands, Athanasios Chatzitakis, Abhijai Velluva, Sarah Geo, Amir Masoud Dayaghi
Lead Participant	UoS
Contributing Participant(s)	UiO
Work Package(s)	WP2
Dissemination Level (PU/SEN)	PU
Nature (R/DEC/DEM/DMP)	R
Version	1.2







## **Document History**

Version	Issue Date	Changes
[1.0]	25.10.2024	Initial draft
[1.1]	30.04.2025	Final version
[1.2]	27.07.2025	Revised version : Fixed header, updated disclaimer text to include CINEA



## **Table of Contents**

1	SUMMARY AND SCOPE
2	OER CATALYST MATERIALS BASED ON BA <sub>0.5-x</sub> SR <sub>0.5-x</sub> CO <sub>0.8-y</sub> FE <sub>0.2+y</sub> O <sub>3-Δ</sub> (BSCF)
3	OER CATALYST MATERIALS BASED ON SR <sub>1-A</sub> (Ti,Fe,M)O <sub>3</sub> (STFM)
	ELECTROCHEMICAL CHARACTERIZATION OF THE SYNTHESIZED BSCF-BASED CATALYSTS IN ROTATING ELECTRODE (RDE)
5	CONCLUSIONS 17





#### 1 Summary and scope

The main scope of this deliverable is to present developments at stage 2 and 3 of catalyst materials for the oxygen evolution reaction (OER) in alkaline environment that will be employed as anodes in Unit 1 (solar-driven alkaline electrolyzer). As a reminder, stage 1 platform materials includes the synthesis and characterization of: i) Ba<sub>0.5-x</sub>Sr<sub>0.5-x</sub>Co<sub>0.8-y</sub>Fe<sub>0.2+y</sub>O<sub>3-δ</sub>-based catalysts (BSCF) and their derivatives with reduced cobalt (Co) contents (e.g. Ba<sub>0.45</sub>Sr<sub>0.45</sub>Co<sub>0.5</sub>Fe<sub>0.5</sub>O<sub>3-δ</sub>), and ii) Sr<sub>1-a</sub>(Ti,Fe,M)O<sub>3</sub> (STFM, M=Fe, Cu, Ni) with no Co. Nevertheless, and for benchmarking purposes, STFNs with low Co contents (around 10% at B-site) will also be synthesized. The design of these catalysts is done by using defect chemistry principles, forming a series of 3-5 members each, to promote the exsolution of surface nanoparticles, to promoted electrochemical activity. After exsolution is succeeded (stage 2 developments), the catalysts are undergoing galvanic replacement reactions (stage 3 developments) with the main aim to replace minimal amounts of the originally exsolved metal nanoparticles with precious and highly electroactive elements such as iridium (Ir) and ruthenium (Ru). The key idea is that the introduction of these heteroatoms and the formation of bi-metallic catalysts will boost the performance compared to the monometallic analogues for the OER in alkaline media. Finally, the systems are characterised compositionally, structurally and electrochemically as benchmarks.

The targeted performance of these catalysts by the end of the project is that they can deliver 50 mA/cm² at an overpotential of 400 mV, i.e. at 1.63 V vs the reversible hydrogen electrode (RHE). Their stability should reach at least 2000 h at near-neutral or alkaline pH. Moreover, a key aim is to minimize or even completely deplete cobalt (Co), but also utilize minimal amounts of precious metals like Ir and Ru to boost their catalytic performance. As it is shown later, we have reached the targeted performance with a certain BSCF variant at stage 2 developments. This is an important milestone, but we need to significantly reduce its Co content, solidify this finding by replicate experiments, as well as assess the long-term stability. In addition, significant are the developments with the STFM-based catalysts, where promising results have already been obtained with much reduced Co contents compared to the BSCF-based catalysts.

#### 2 OER catalyst materials based on Ba<sub>0.5-x</sub>Sr<sub>0.5-x</sub>Co<sub>0.8-y</sub>Fe<sub>0.2+y</sub>O<sub>3-δ</sub> (BSCF)

The BSCF-based catalysts were synthesized by the sol-gel citrate method in which the nitrate precursors and barium carbonate (BaCO<sub>3</sub>) are mixed and treated to form a gel, which is combusted at 250°C. The obtained ash is then fired at 450°C and finally calcined at 1100°C. The main synthetic steps are given in Figure 1.





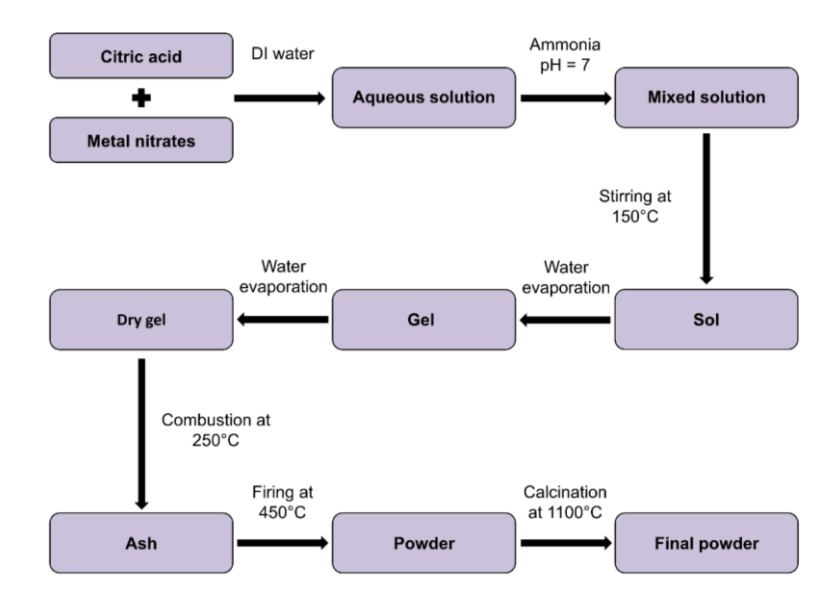


Figure 1: Synthesis steps of the sol-gel citrate method used to synthesize the BSCF-based catalysts.

By following this methodology, we have currently synthesized the following compositions, where a reduction in the Co content has been implemented.

**Table 1:** Composition of the BSCF-based catalysts designed and synthesized with their respective abbreviations and nominal B-site substitution

Stoichiometric composition	Abbreviation	Nominal substitution / comment
Ba <sub>0.5</sub> Sr <sub>0.5</sub> Co <sub>0.8</sub> Fe <sub>0.2</sub> O <sub>3-δ</sub>	BSCF82	Base material, B-site: 20% Fe
Ba <sub>0.45</sub> Sr <sub>0.45</sub> Co <sub>0.8</sub> Fe <sub>0.2</sub> O <sub>3-δ</sub>	BSCF82-10AD	10% A-site deficiency, B-site: 20% Fe
Ba <sub>0.475</sub> Sr <sub>0.475</sub> Co <sub>0.8</sub> Fe <sub>0.2</sub> O <sub>3-δ</sub>	BSCF82-5AD	5% A-site deficiency, B-site: 20% Fe
Ba <sub>0.475</sub> Sr <sub>0.475</sub> Co <sub>0.8</sub> Fe <sub>0.2</sub> O <sub>3-δ</sub>	BSCF82-5AD	5% A-site deficiency, B-site: 20% Fe / annealed at 900 °C
Ba <sub>0.5</sub> Sr <sub>0.5</sub> Co <sub>0.6</sub> Fe <sub>0.4</sub> O <sub>3-δ</sub>	BSCF64	B-site: 40% Fe
Ba <sub>0.475</sub> Sr <sub>0.475</sub> Co <sub>0.6</sub> Fe <sub>0.4</sub> O <sub>3-δ</sub>	BSCF64-5AD	5% A-site deficiency, B-site: 40% Fe

All BSCF-based catalysts have been characterized by scanning electron microscopy (SEM) and X-ray diffraction (XRD) in order to observe and verify their structure and crystallinity. The SEM and XRD results are given below.



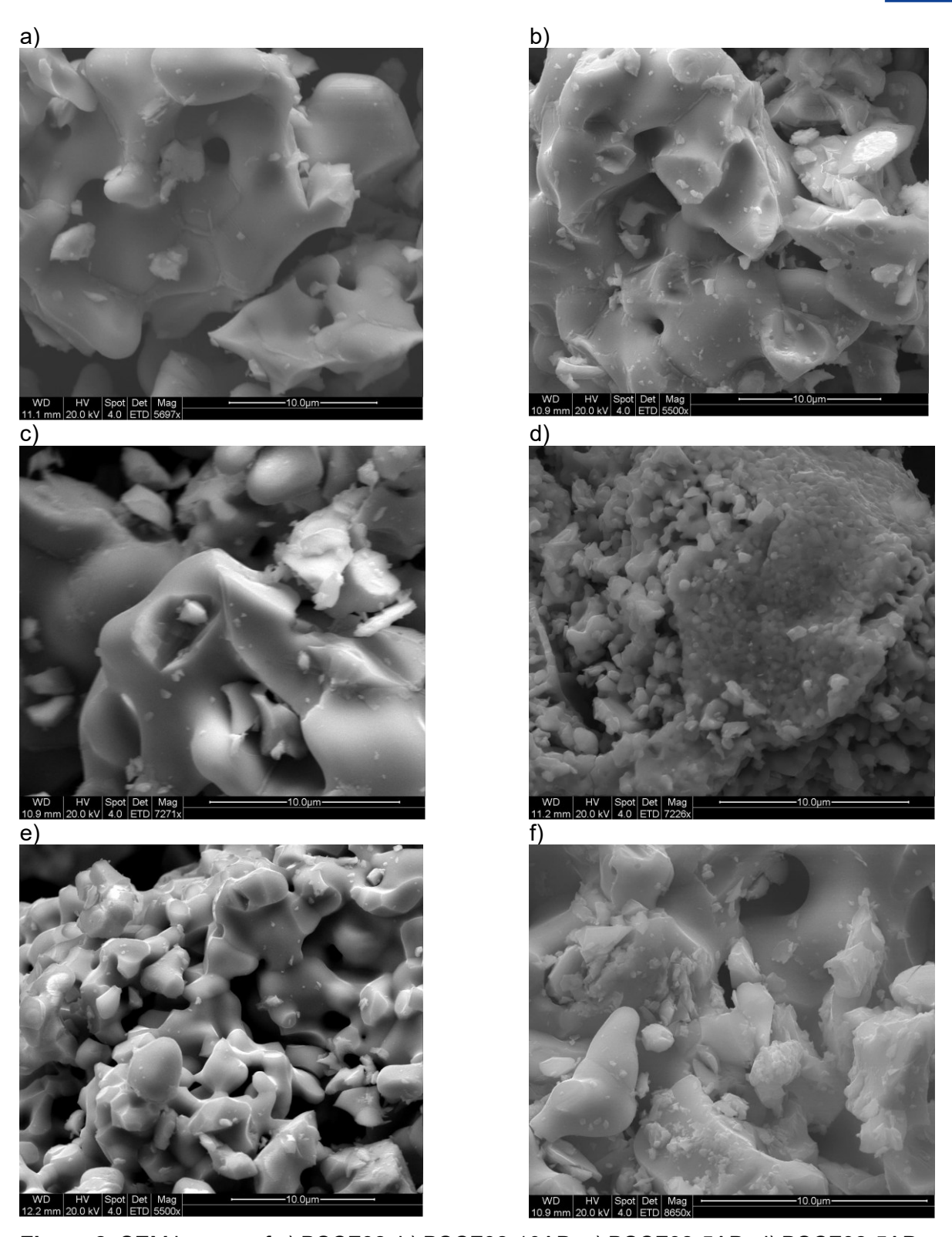


**Figure 2:** SEM images of a) BSCF82, b) BSCF82-10AD, c) BSCF82-5AD, d) BSCF82-5AD annealed at 900°C, e) BSCF64, f) BSCF64-5AD.

All BSCF82-based catalysts appear to have the same granular morphology with grain sizes in the range of a few micrometers, with the exception of BSCF82-5AD that was annealed at 900°C. As the annealing temperature was lowered, it was expected that the grain sizes would decrease, and appear to be in the



range of 1 μm. Lowering the Co content in BSCF64 it also appears to decrease somewhat the grain sizes, but they are still in the range of a few μm. The XRD diffractograms are presented in Figure 3.

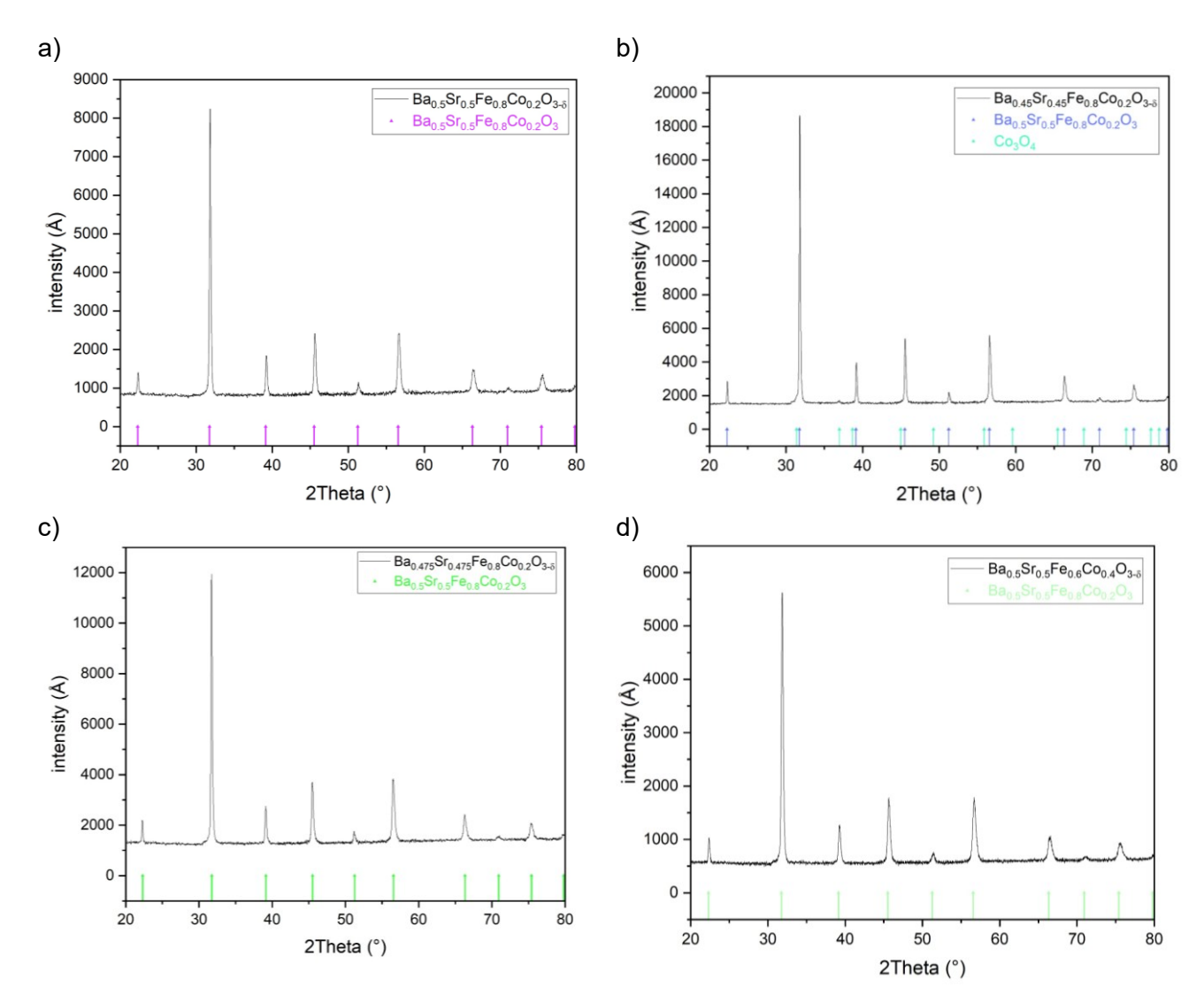


Figure 3: XRD diffractograms of a) BSCF82, b) BSCF82-10AD, c) BSCF82-5AD and d) BSCF64.

The XRD patterns of BSCF82-5AD that was annealed at 900 °C and of BSCF64-5AD are identical to BSCF82-5AD annealed at 1100°C (c) and BSCF64 (d), respectively. The XRD patterns confirm the successful synthesis of all the samples, as well as their high degree of crystallinity. All samples appear to be single phase except for a small amount of a secondary phase of  $Co_3O_4$  in BSCF82-10AD.

The elemental composition of the BSCF-based catalysts was studied by energy dispersive spectroscopy (EDS). The results are given in Figure 4.



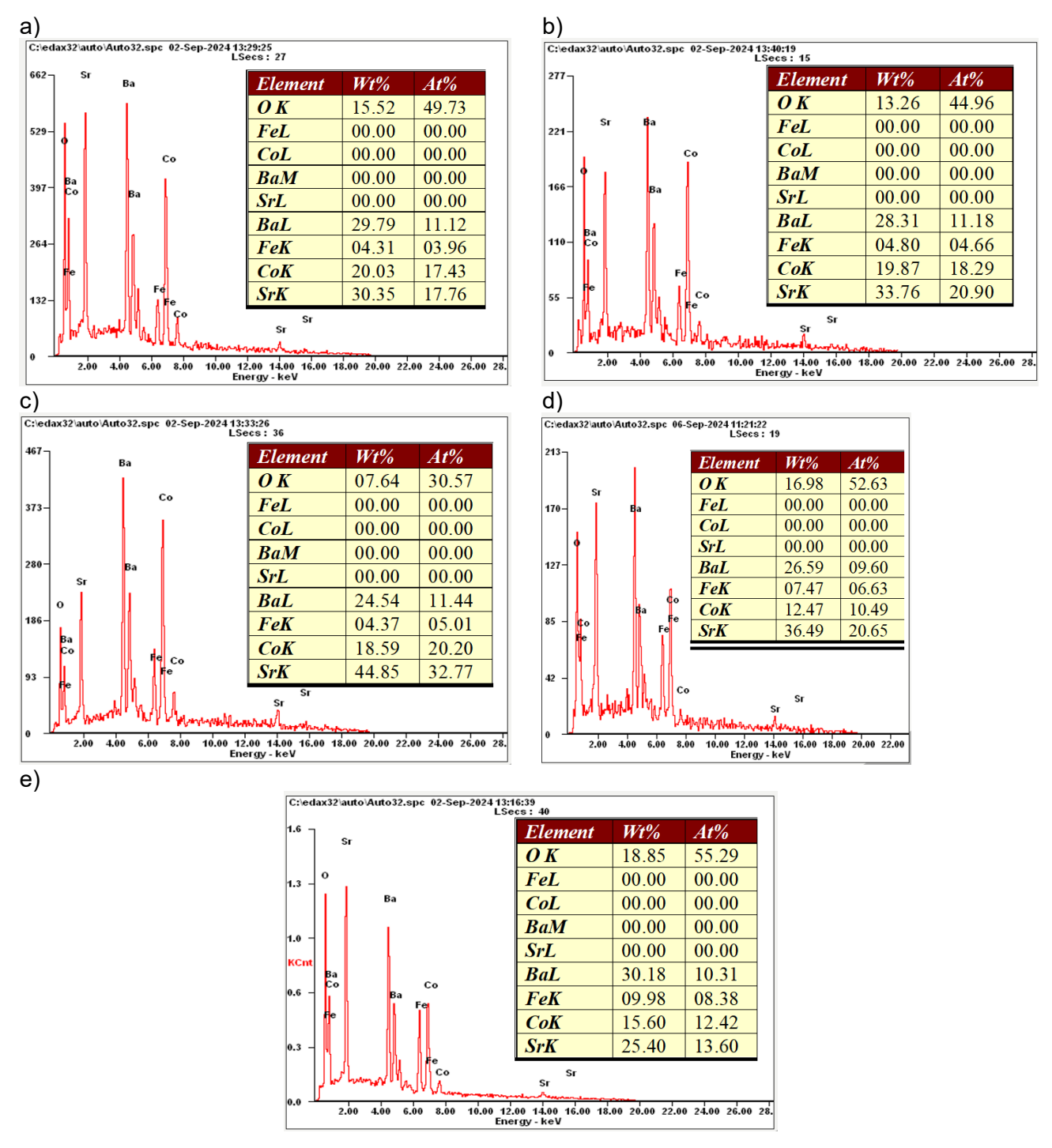


Figure 4: EDS spectra of a) BSCF82, b) BSCF82-10AD, c) BSCF82-5AD, d) BSCF64, e) BSCF64-5AD

The EDS analysis shows that the samples do not contain any impurities and all the expected elements are present (Ba, Sr, Co and Fe). It is important to notice that the Co/Fe atomic weight precent (At%) ratio correlates well with the expected ratio from the nominal compositions in BSCF82 (4/1) and BSCF64 (3/2). This further showcases the successful synthesis of the different BSCF-based catalysts.

The A-site deficiency is important in order to engineer the materials for exsolution of the B-site cations, according to the following equations.





Eq. 1

Eq. 2

$$ABO_{3-\delta} \xrightarrow{exsolution} (1-a)ABO_{3-\delta}$$
,  $+aAO + aB$  (reducing conditions)  
 $A_{1-a}BO_{3-\delta lim} \xrightarrow{exsolution} (1-a)ABO_{3-\delta} + aB$  (reducing conditions)

For this, we have performed thermogravimetric analysis (TGA) of stoichiometric and A-site deficient BSCFs in 5% H<sub>2</sub> in Ar (HArmix) atmosphere to better study the exsolution process and find the best conditions for the reaction to occur. Representative TGA curves for stoichiometric and 5% A-site deficient BSCFs can be seen in Figure 5.

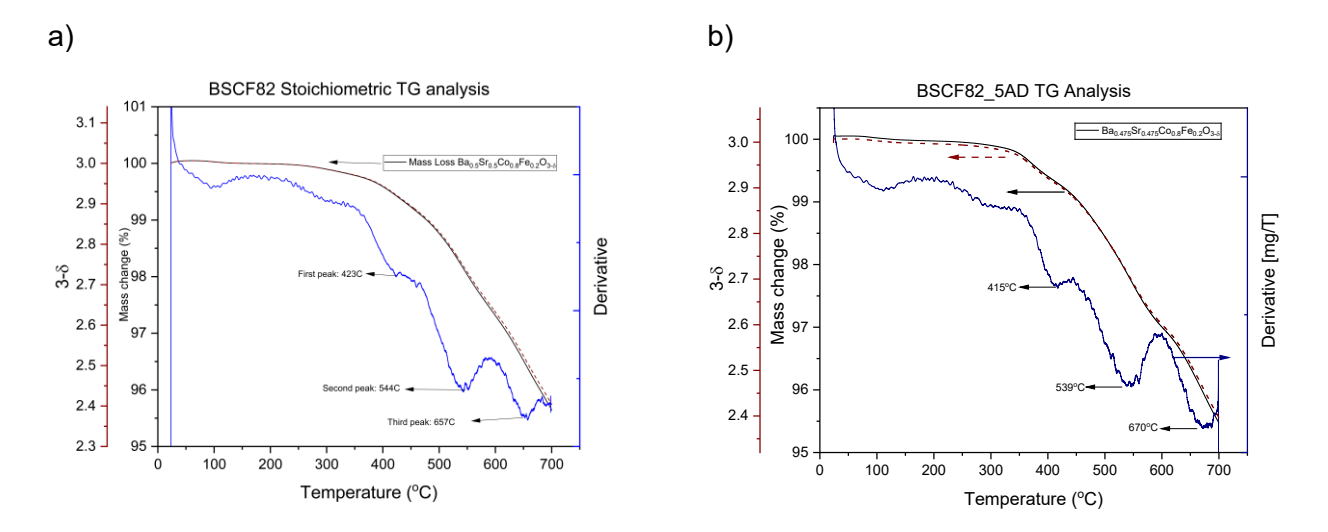


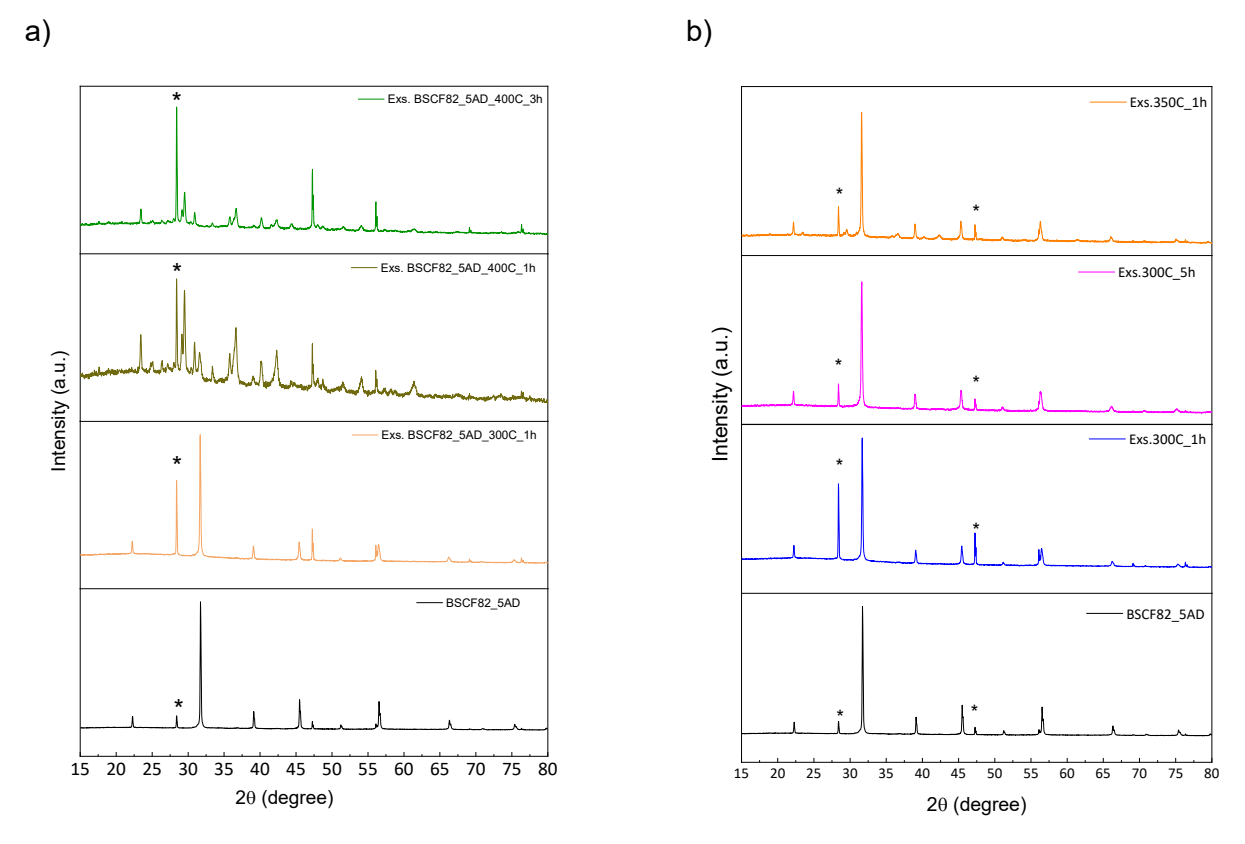
Figure 5: TGA curves of a) stoichiometric BSCF82 and b) 5% A-site deficient BSCF82 in HArmix.

Based on the derivative curves in the TGA curves of Figure 5, both samples display three main reduction steps. The first reduction happens at 423 and 415°C for the stoichiometric and 5% A-site deficient BSCFs, respectively. It is noted that Co and Fe follow different redox pathways and may be reduced at distinct temperatures. Further analysis, such as in-situ XRD and EXAFS (to be planned in WP4 and operando studies), is required to accurately identify these reduction steps. Finally and from these TGA curves, we also speculate that Ruddlesden-Popper phases and metallic exsolved Co are being formed during reduction temperatures of up to 700°C.

We have then chosen to perform the exsolution process at somehow lower temperatures than the first reduction step, at 300, 350 and 400°C for 1, 3 or 5 h in HArmix. The XRD analysis in Figure 6 clearly indicates that above 350°C, secondary phases appear, but also the main peak at approx. 31.8° 2theta disappears, indicating the complete degradation of the material. These results are in good agreement with the TGA curves, where we see that we have significant oxygen loss after approx. 350°C.

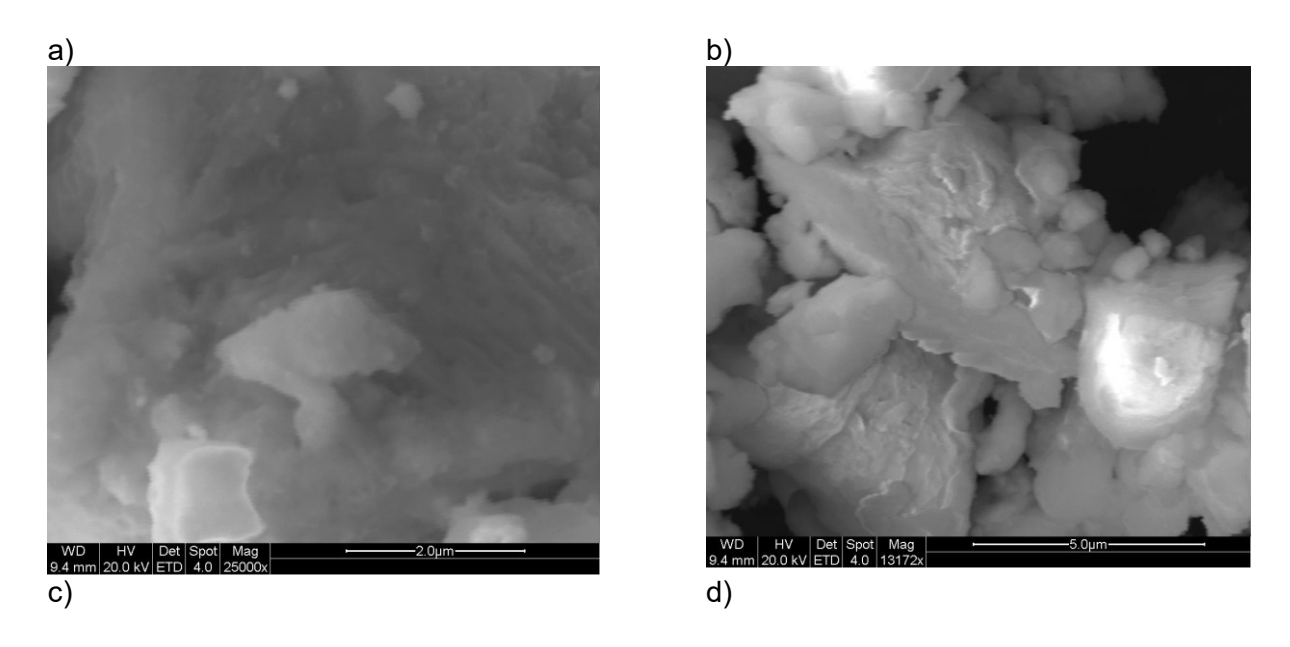






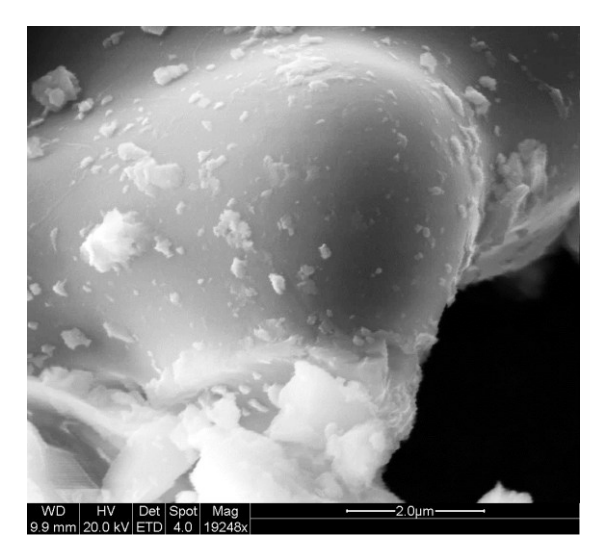
**Figure 6:** XRD graphs of 5% A-site deficient BSCFs at different annealing temperatures and times in HArmix.

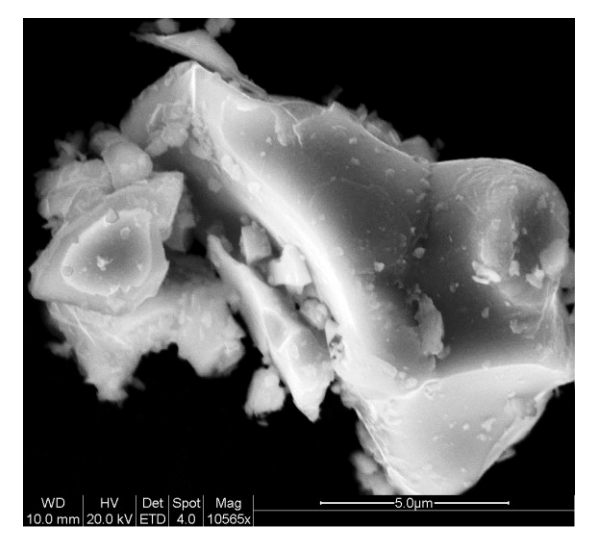
This can also be seen from the change in the surface morphology in the following SEM images of Figure 7.







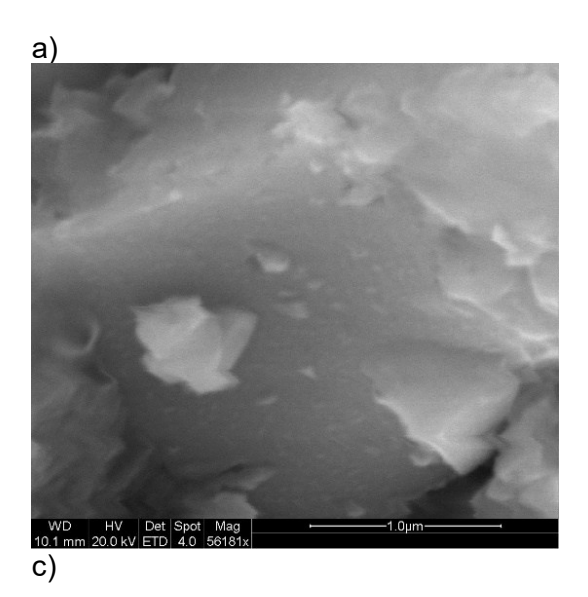


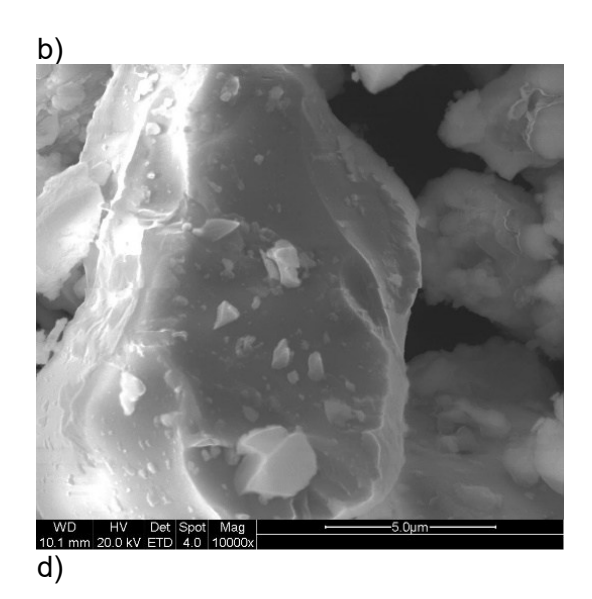


**Figure 7:** SEM images of a) and b) 5% A-site deficient BSCF annealed in HArmix at 400°C for 1 h and c) and d) 5% A-site deficient BSCF annealed in HArmix at 300°C for 5 h.

From Figure 7 it is evident the distorted morphology of the BSCFs treated at 400°C (Figure 7a and b) even for 1 h, compared to the samples treated at 300°C for 5 h (Figure 7c and d). In the latter, the large crystals are retained and are decorated with intrinsic particles in the range of micrometres, as well as exsolved nanoparticles in the range of a few nanometres.

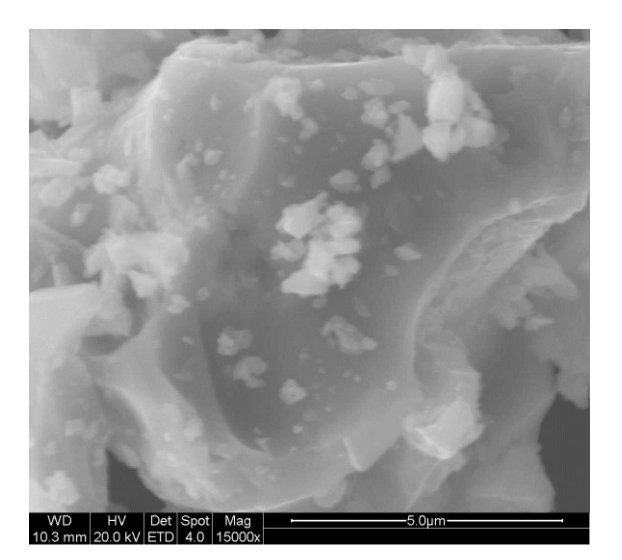
Therefore, 350°C is the maximum temperature for optimum exsolution in the BSCF system of catalysts and below we show some indicative SEM images (Figure 8) of exsolved nanoparticles on A-site deficient BSCFs at 300 and 350°C.

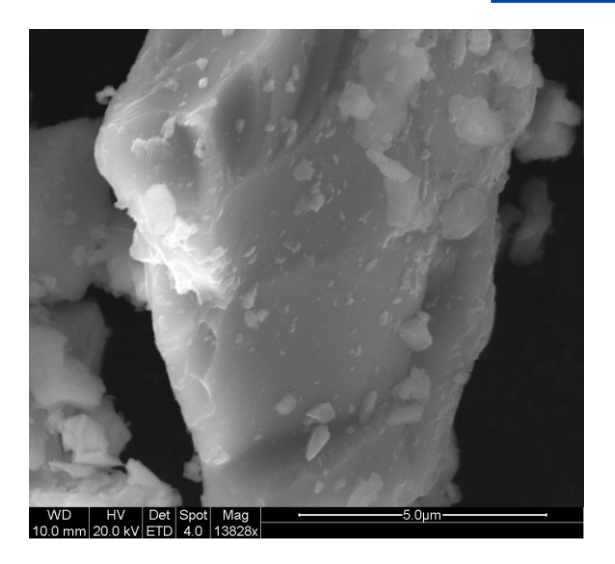






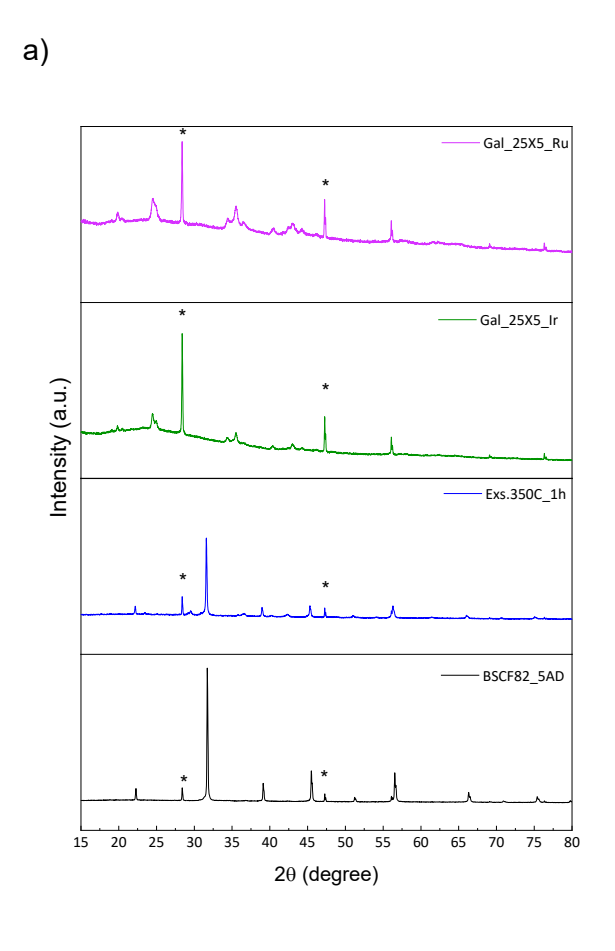






**Figure 8:** SEM images of 5% A-site deficient BSCF annealed in HArmix a) and b) at 350°C for 1 h and c) 300°C for 1 h and d) 5% A-site deficient BSCF annealed in HArmix at 300°C for 5 h.

In stage 3, the exsolved catalysts are galvanically replaced with Ir or Ru heteroatoms with the main aim to form bimetallic exsolved nanoparticles, improving the electrocatalytic activity for the OER. In our initial experimental conditions, the galvanic replacement reaction occurred in 0.1 M  $HCIO_4$  aqueous solutions containing 1 mM  $K_2IrCI_6$ , or 1 mM  $RuCI_3$ , which are the sources of Ir and Ru atoms, respectively. At these conditions, we observed the degradation of our BSCFs from both XRD and SEM as seen below.



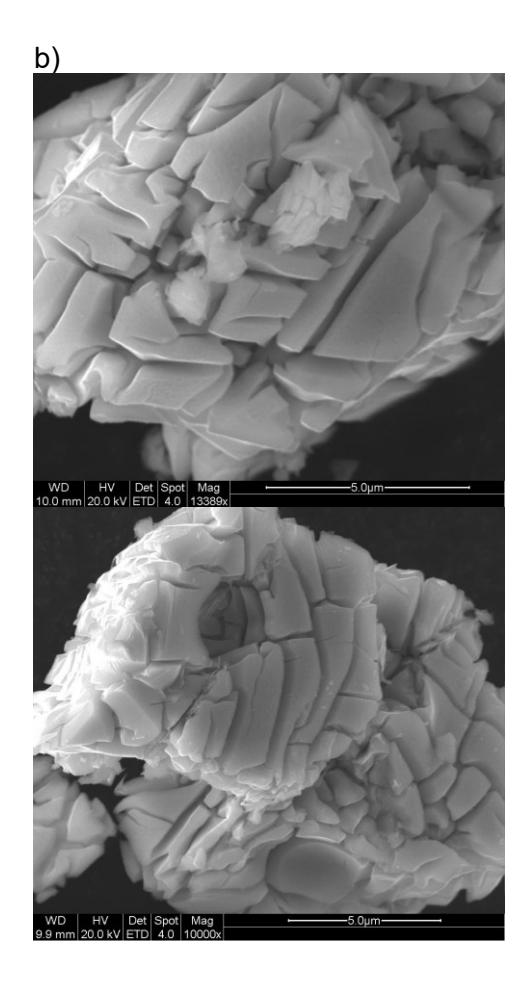






**Figure 9:** a) XRD graphs of 5% A-site deficient BSCF (BSCF82\_5AD) annealed in HArmix at 350°C for 1 h (Exs.350C\_1h) and galvanically replaced at 25°C for 5 min in 1 mM K<sub>2</sub>IrCl<sub>6</sub> (Gal\_25x5\_Ir), or 1 mM RuCl<sub>3</sub> (Gal\_25x5\_Ru), showing the disappearance of main BSCF peaks (e.g. 31.8°, 45.3°). b) SEM images of the Gal\_25x5\_Ir sample, showing severe morphological changes.

Figure 9 shows the corrosive effect of 0.1 M HClO<sub>4</sub> on the surface of BSCF and for this reason we are currently performing galvanic replacements in less acidic solutions like 1 mM HCl and even in basic ones, such as 1 M KOH (pH = 14). It seems that such a modification helped retaining the morphology of the perovskite, on the other hand, a variety of deposits appear on the surface of the exsolved BSCFs.

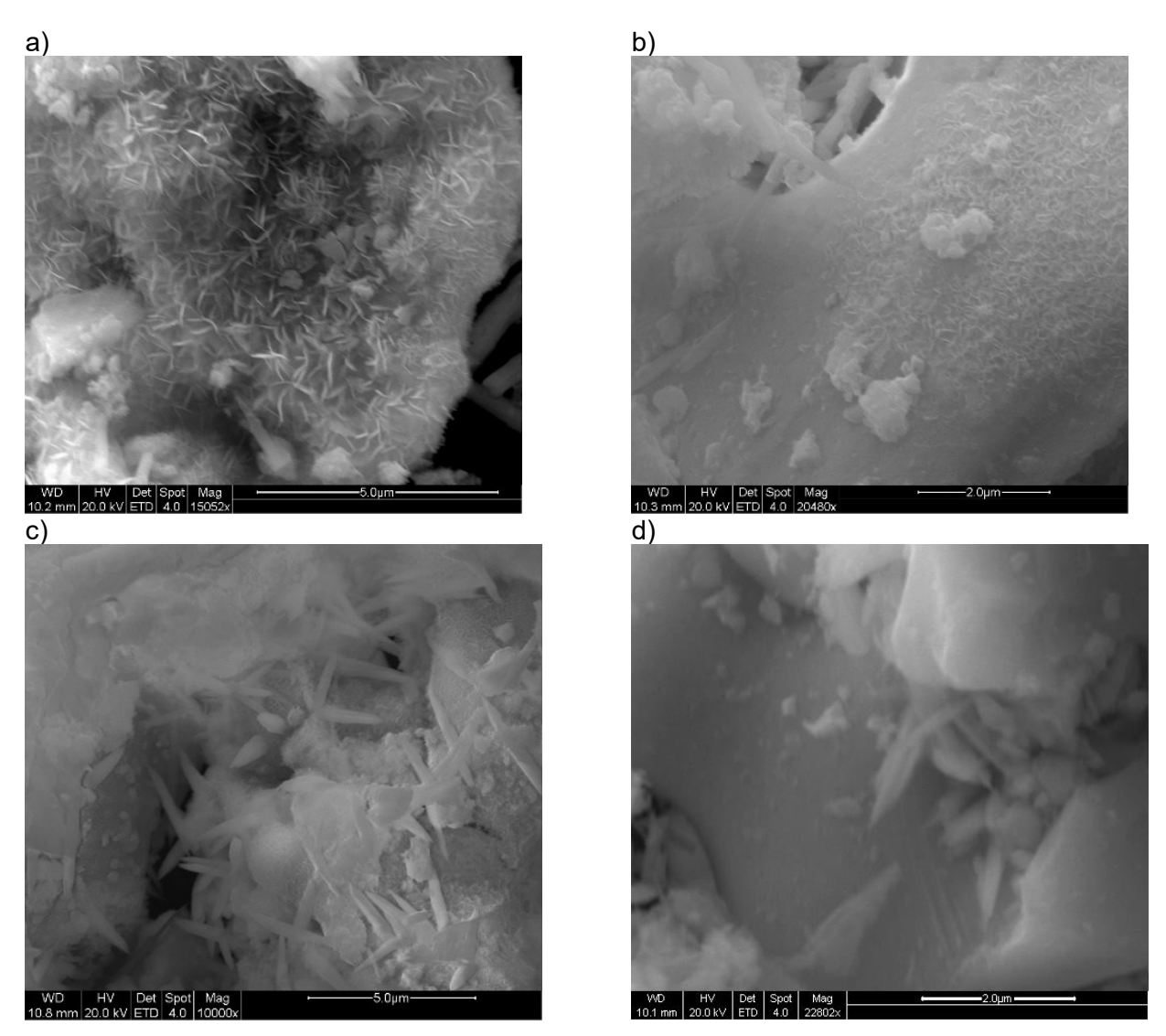


**Figure 10:** Galvanic replacement of exsolved, either at 300 or 350°C, BSCFs in a) 1 mM  $K_2IrCl_6$  in 1 M KOH (ph 14), b) 1 mM  $K_2IrCl_6$  in KOH (pH 12), c) 1 mM  $K_2IrCl_6$  in KOH (pH 8) and d) 1 mM RuCl<sub>3</sub> in 1 mM HCl (pH 3). The temperature in the galvanic reaction step was either at 25, or 40 or 60°C.

We see that morphology of the perovskite is retained (Figure 10) but the deposits have the form of nanoneedles and/or nanosheets/nanocorals. This is not the expected morphology as these deposits cover the exsolved nanoparticles and significant part of the surface of the perovskite, therefore we expect that the OER activity will be worsen. This is indeed the case as it will be shown later in the electrochemical activity of these catalysts.



We are already modifying our protocols and a key modification will be the decrease in concentration of the noble metal salt in the solution, as well as temperature and reaction time. We foresee that going to concentrations down to 10<sup>-6</sup> M and reaction times in the range of seconds could help, by reducing the amount of deposits. Currently, we believe that the high concentration of the noble metal salt and time of reaction, leads to overgrowth of the noble metal particles on the surface of the exsolved BSCFs. Finally, high-resolution transmission electron microscopy (TEM) and X-ray Photoelectron Spectroscopy (XPS) studies are planned to further characterize the surface of the catalysts and composition of the exsolved nanoparticles, as well as deposits after the galvanic replacement step.

#### 3 OER catalyst materials based on Sr<sub>1-a</sub>(Ti,Fe,M)O<sub>3</sub> (STFM)

In D2.1 we reported the synthesis of STFM-based catalysts (M = Fe, Ni, Cu, Co) using a modified solid-state method. In our previous deliverable (D2.1), we demonstrated that traditional solid-state synthesis methods for STFM-based perovskite materials produced catalysts with significant limitations for OER applications. The solid-state route resulted in the formation of very large grains, which inherently restricted catalytic performance due to limited surface area. As evidenced by the SEM images in D2.1, these large crystallites (ranging from ~0.5-3 µm for STFM compositions) imposed considerable diffusion length-scales for exsolvable species, significantly hindering the exsolution process that is critical for creating highly active catalytic surfaces. The combination of low surface area and impaired exsolution capability directly translated to suboptimal OER activity in the resultant materials. However, our Co variant, even in solid state synthesised form was competitive with the reference BSCF systems.

We are pleased to report significant progress in advancing an alternative synthesis route that effectively addresses these limitations. Our research team has developed and optimized a sol-gel combustion method that produces STFM perovskites with substantially improved morphological and functional characteristics. This approach utilizes metal nitrate precursors combined with citric acid as both a chelating agent and fuel. The process begins with the mixing of precursors and fuel, followed by gelation, combustion/ignition, firing, grinding to powder, and finally calcination. This methodology has been successfully applied to produce STFCo perovskites with reduced cobalt content.

**Table 2:** Composition of the STFM-based catalysts designed and synthesized with their respective abbreviations and nominal B-site substitution

Stoichiometric composition	Abbreviation	Nominal substitution / comment
$Sr_{0.95}Ti_{0.3}Fe_{0.7}O_3-\gamma$	Sr95TF3070	5% A-site deficiency, B-site: 30% Ti, 70% Fe
$Sr_{0.95}Ti_{0.3}Fe_{0.6}Cu_{0.1}O_3$ - $\gamma$	Sr95TFC306010	5% A-site deficiency, B-site: 30% Ti, 60% Fe, 10% Cu
$Sr_{0.95}Ti_{0.3}Fe_{0.6}Ni_{0.1}O_3-\gamma$	Sr95TFN306010	5% A-site deficiency, B-site: 30% Ti, 60% Fe, 10% Ni
$Sr_{0.95}Ti_{0.3}Fe_{0.6}Co_{0.1}O_{3}-\gamma$	Sr95TFCo306010	5% A-site deficiency, B-site: 30% Ti, 60% Fe, 10% Co
$Sr_{0.95}Ti_{0.3}Fe_{0.65}Co_{0}.05O_{3}-\gamma$	Sr95TFCo306505	5% A-site deficiency, B-site: 30% Ti, 65% Fe, 5% Co

Our first significant advancement has been the optimization of the sol-gel synthesis protocol specifically tailored for STFM perovskites with reduced cobalt content. Initial investigations revealed that SrCO<sub>3</sub> formation was a persistent challenge in conventional synthesis approaches, negatively impacting phase purity and likely the catalytic performance. We successfully addressed this issue by prolonging the firing stage, which effectively suppressed secondary phase formation. The extended protocol involves initial





heating at 400°C for 2 h, followed by an additional furnace firing at 400°C for 8 h before final calcination at 800-1000°C. XRD analysis confirmed that samples produced with this extended firing stage demonstrate significantly higher phase purity, as evidenced by the elimination of SrCO<sub>3</sub> peaks in the diffraction patterns (Figure 11). This refined approach represents a substantial improvement over the solid-state method used previously, enabling the production of phase-pure perovskites with controlled morphology essential for optimal oxygen evolution reaction activity.

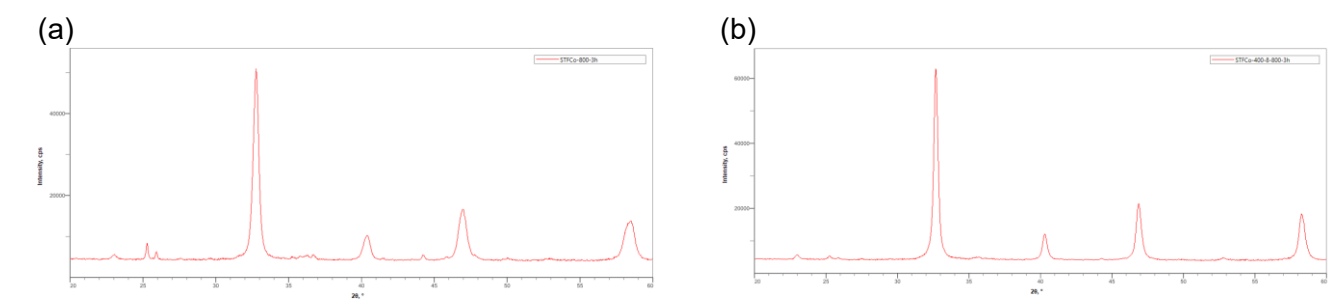


**Figure 11:** XRD patterns comparing STFCo synthesis methods. (a) Standard sol-gel process with initial firing at 400°C for 2 h followed by calcination at 800°C for 3, showing minor secondary phase impurities. (b) Optimized sol-gel process with extended firing at 400°C for 8 before calcination at 800°C for 3, demonstrating significantly improved phase purity with elimination of SrCO<sub>3</sub> peaks.

Our second major advancement focuses on the optimization of calcination conditions to achieve both high phase purity and improved energy efficiency. Through systematic investigation of calcination temperatures and durations for STFC, STFCo, and STFN compositions, we identified optimal parameters that significantly reduce energy consumption without compromising material quality. XRD analysis of STFC samples calcined at temperatures ranging from 600°C to 1000°C revealed that phase-pure perovskites could be obtained at lower temperatures than previously employed, with near-complete phase formation achieved at 900°C for just 3 rather than the standard 6 (see Figure 12). Quantitative energy consumption analysis demonstrated that this revised protocol reduces electrical energy requirements by approximately 40% compared to solid state synthesis, with a corresponding decrease in manufacturing costs. This approach also allowed us to prepare a Co-based composition with even lower Co amount, Sr95TFCo306505 (see Figure 13).

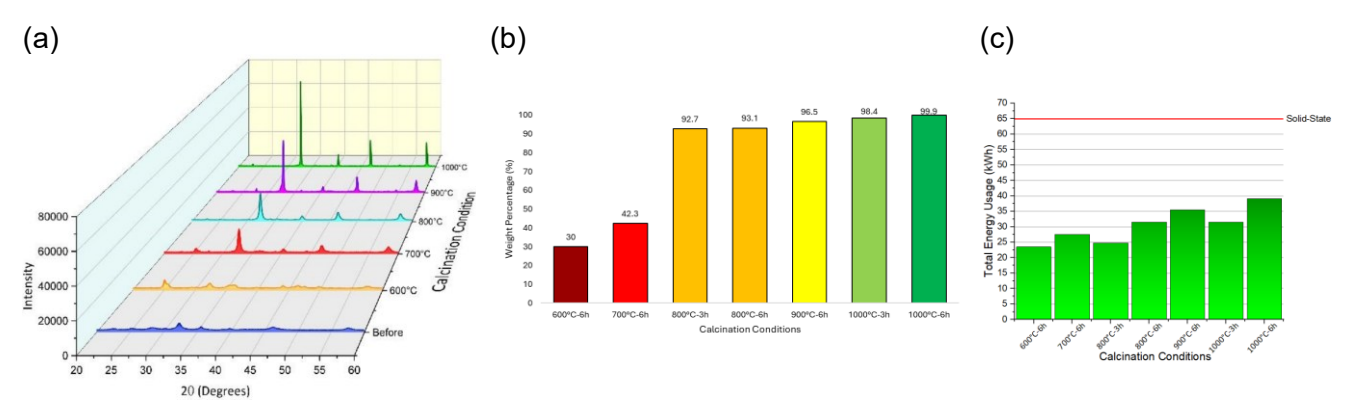


**Figure 12:** Optimization of calcination parameters for perovskite synthesis. (a) 3D representation of XRD patterns for STFC samples calcined at temperatures from 600°C to 1000°C, showing progressive phase development. (b) Samples purity as a function of calcination conditions. (c) Comparative analysis of phase purity and approximate electric energy consumption between sol-gel and conventional solid-state synthesis methods.



Our third key advancement involves establishing quantitative relationships between synthesis parameters and the resulting microstructural characteristics of STFM perovskites. Through Rietveld refinement of XRD data collected from our calcination optimization studies, we identified clear trends in crystallite size and microstrain as functions of processing temperature and time. The results reveal an inverse relationship between crystallite size and microstrain across the temperature range of 600-1000°C, with crystallite size increasing from approximately 0.2 µm at 600°C to 1.4 µm at 1000°C, while microstrain decreases mulitfold. Note that the purity also varies (Figure 12b). This insight provides a powerful tool for tailoring material properties, as smaller crystallites with higher microstrains offer enhanced surface area and improved exsolution capabilities. Notably, the sol-gel synthesized samples consistently demonstrate significantly smaller crystallite sizes and higher microstrain values compared to analogous materials prepared via solid-state methods, creating microstructures more favourable for catalytic applications while using less energy-intensive processing conditions.

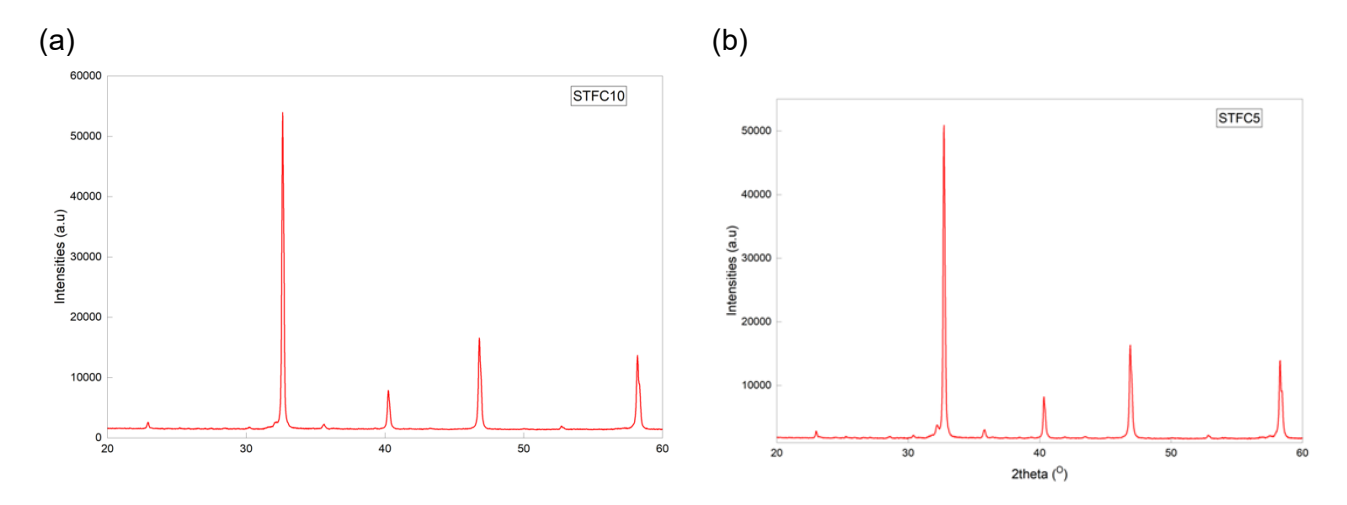


**Figure 13:** XRD patterns for STFCo sample after calcination at 1000°C (3 h) for (a) Sr95TFCo306010 and (b) Sr95TFCo306505.

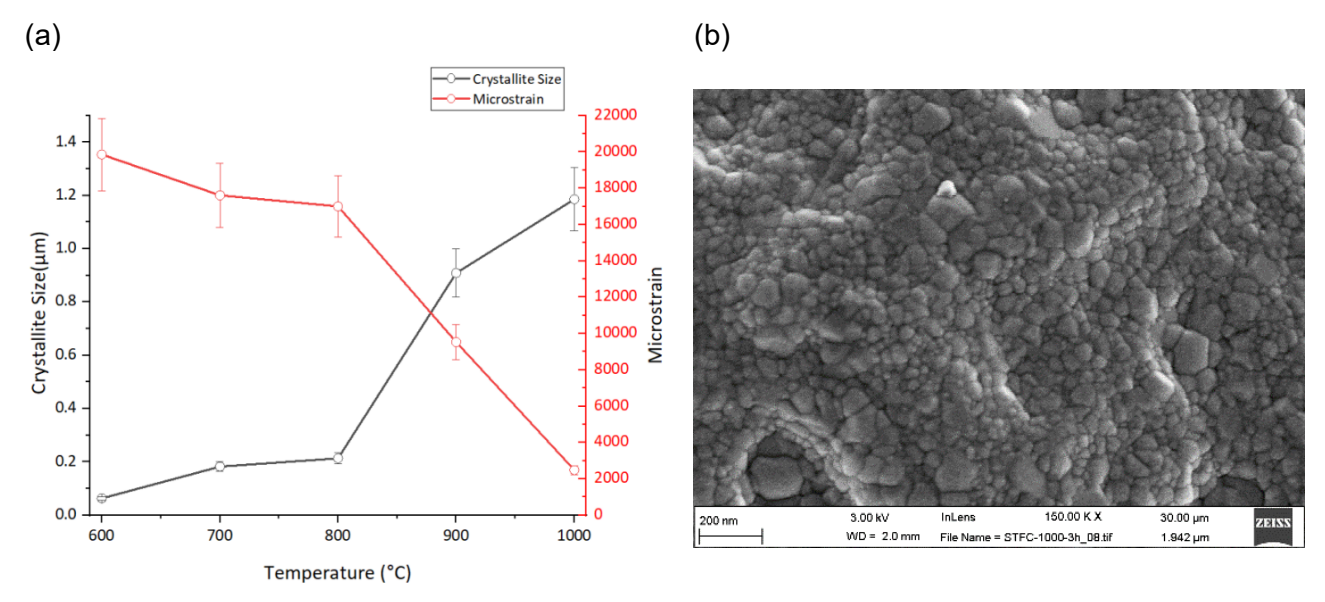


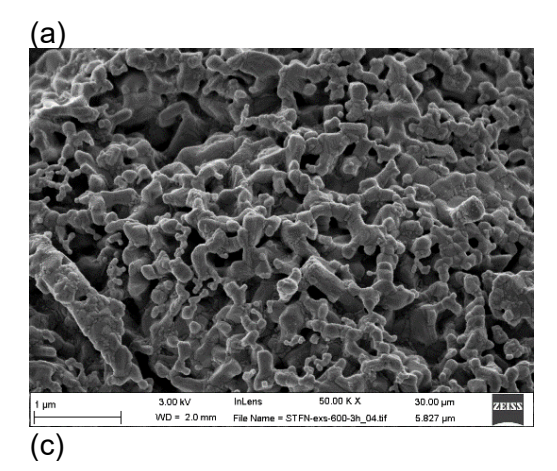
Figure 14: Relationship between synthesis conditions and microstructural properties. (a) The graph shows crystallite size (blue line, left axis) and microstrain (red line, right axis) as functions of

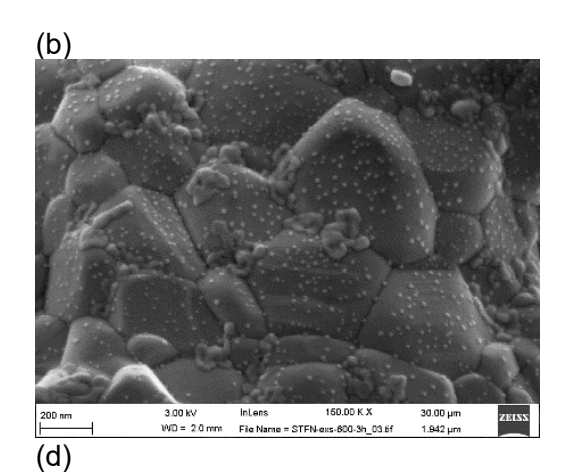


calcination temperature for STFC perovskites, with (b) SEM images confirming the nanoscale morphology at optimal processing conditions.

Our fourth significant advancement concerns the test of exsolution conditions to produce well-distributed, catalytically active nanoparticles on perovskite surfaces. We discovered that reducing temperatures of 400-600°C under 5% H<sub>2</sub>/Ar atmosphere yield superior exsolution characteristics compared to more aggressive reduction regimes previously employed, with energy consumption reduction benefits. SEM imaging reveals that all three perovskite compositions (STFC, STFN, and STFCo) exhibit excellent early-stage surface activity with distinctive nanoparticle formation patterns. The moderate temperature approach produces finely distributed nanoparticles (5-40 nm) while preserving the underlying perovskite structure and avoiding the detrimental sintering and overgrowth effects observed at higher temperatures (Figure 15). This controlled exsolution technique creates catalyst surfaces with high active site density while minimizing energy input, representing a significant step toward more sustainable catalyst fabrication. Notably, these results suggest that effective nanoparticle formation can be achieved even in compositions with substantially reduced cobalt content, offering a promising pathway for developing high-performance, environmentally responsible OER catalysts.

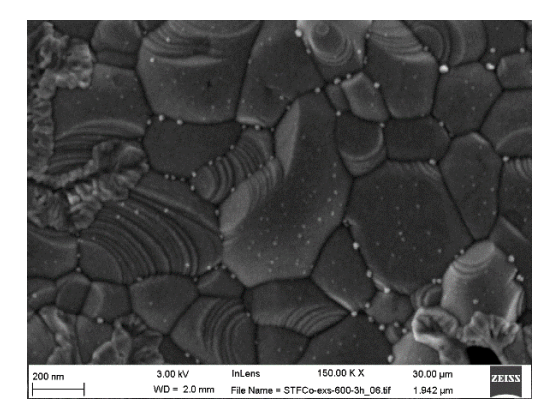
Having successfully developed these optimized synthesis and exsolution protocols for STFM perovskites with reduced cobalt content, we are now preparing to evaluate their performance as OER catalysts. The electrochemical testing apparatus is currently in the final stages of setup and calibration at the facilities in UoS, that will enable comprehensive assessment of catalytic activity, stability, and selectivity under conditions relevant to alkaline water electrolysis. Based on our microstructural characterization and the promising results previously observed with STFCo variants in D2.1, we anticipate that these sol-gel synthesized materials will demonstrate significant improvements in OER performance compared to their solid-state counterparts, while maintaining substantially reduced dependence on cobalt. The combined benefits of enhanced surface area, optimized exsolution behaviour, and improved phase purity should translate into higher catalytic activity, potentially approaching our target of 50 mA/cm² at 400 mV overpotential. These upcoming electrochemical evaluations will provide crucial data for further refinement of our materials design strategy, ultimately contributing to the development of sustainable, high-performance catalysts for renewable energy applications.











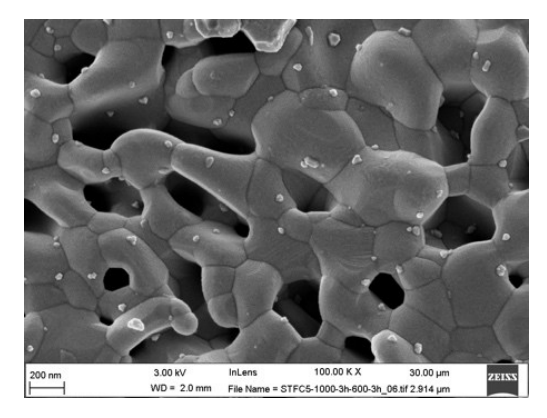
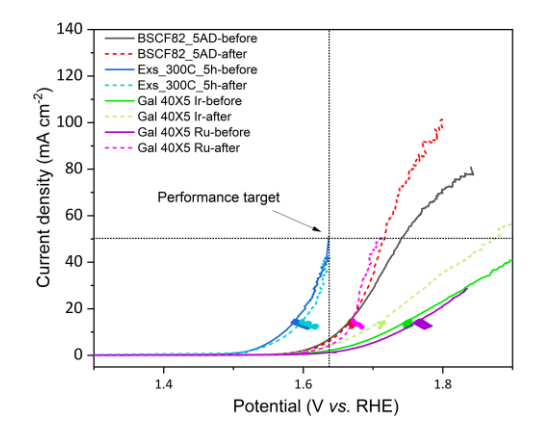


**Figure 15:** SEM micrographs demonstrating controlled nanoparticle exsolution on perovskite surfaces. (a-b) Images show the evolution of surface morphology for STFN after exsolution at 600°C for 3 h, revealing well-defined nanoparticles uniformly distributed across the grain structure at different magnifications. (c) Sr95TFCo306010 (10% Co) and (d) Sr95TFCo306505 (5% Co).

# 4 Electrochemical characterization of the synthesized BSCF-based catalysts in rotating disc electrode (RDE)

In all cases and before electrochemical characterization, the RDE with as deposited catalyst was cleaned electrochemically by performing cyclic voltammetry (CV) between 0.7 and 1.2 V vs. RHE at 50 mV/s until steady-state conditions were obtained. Subsequently, the catalyst was activated by CV at a scan rate of 10 mV/s from the non-Faradaic region to the potential required to reach a current density of 10 mA/cm². After 10 cycles of activation, most catalyst materials showed a steady-state behaviour. Then, linear sweep voltammograms (LSVs) were recorded to typically 1.9 V vs RHE. A few representative results are given in Figure 16.





Sample	η <sub>50</sub> (mV) – <i>iR</i> corrected
BSCF_5AD	480
Exs.300C_5h	400
Gal_40X5_Ir	650
Gal_40X5_Ru	N/A

**Figure 16:** a) Current-voltage curves of BSCF-based catalysts with A-site deficiency, exsolution and subsequent galvanic replacement reaction with Ir and Ru. b) Activity table showing the overpotential at 50 mA/cm², which is the targeted performance of Unit 1. All measurements were conducted in a rotating disc electrode (RDE) configuration in a three-electrode set up in 1 M KOH. A carbon rod and a Hg/HgO electrode were used as counter and reference electrodes, respectively. Scanning rate was 10 mV/s under continuous O₂ bubbling. The catalyst loading in all cases was 0.28 mg/cm² nominal RDE area.





According to the set targets in the project, we aim at producing 50 mA/cm² at 400 mV overpotential, i.e. at 1.63 V vs RHE. Currently, we observe that the exsolved at 300°C for 1 h, 5% A-site deficient BSCF82 has reached the set target for Unit 1. See Figure 16a and blue curves therein. This means that even at stage 2 of the catalyst materials we have reached the project target. Nevertheless, we are now performing a series of multiple experiments to solidify and further confirm this result. On the other hand, BSCF82 contains 80% Co in the B-site, which accounts for almost the 20% of the whole perovskite structure and this is a significant amount for Co. As soon as we confirm the performance of our catalyst in multiple runs, we will pursue its significant reduction in BSCF.

#### 5 Conclusions

In conclusion, and in the case of the BSCF-based platform catalyst materials, we have already reached the project target of 50 mA/cm² and at an overpotential of 400 mV with 5% A-site deficient BSCF82 exsolved at 300°C for 1 h. It is extremely important now to confirm this activity by multiple experiments of synthesis and characterization of the specific catalyst and then investigate the decrease in the Co content without compromising the activity of the catalyst. The materials selection study in WP14 and especially the deliverable WP14.1, showed that the most promising catalysts in terms of environment, cost, toxicity and social acceptance are based on SrTiO<sub>3</sub> (STO). In the same study, BSCF scores somewhere in the middle (5<sup>th</sup> out of 10), therefore by reducing its Co content can become a good alternative, considering its high activity.

Future work includes the extensive electrochemical and physicochemical characterization, as well as long stability testing of the most promising BSCF in parallel with its Co content reduction. The stage 3 developments that include the galvanic replacement reaction will still be followed until the expected morphology is obtained that will be indicative of the activity of the introduction of noble metal elements. such as Ir and Ru. We still believe that these can have a positive effect, boosting the performance further. As mentioned, in the galvanic replacement step we will investigate the concentration of the Ir or Ru precursor in the reaction solution, as well as the reaction time and temperature. We foresee that concentrations down to 10<sup>-6</sup> M and reaction times in the scale of seconds at room temperature or higher can give us the expected morphology change, i.e. modification of the exsolved nanoparticles locally, rather than significant deposits all over the surface of the perovskite. Nevertheless, if the targeted activity is reached without the galvanic replacement step, then such developments will be prioritized and the galvanic replacement step for BSCFs may be dropped. Such an assessment will be conducted at M24, when a mid-term risk assessment and overall project performance will be conducted by UiO. Additionally, STO-based materials with as low as 3 wt% in Co have also shown very promising OER activity, with the study of WP14 placing them as the second best alternative after STO modified with iron (Fe) alone (STF). Additional developments at stage 2 and 3 for the STFs are also ongoing and expected to provide us with good, if not better alternatives for BSCF.

Regarding the long-term stability of the catalysts, this will be done stepwise. We will start with tests exceeding the 100 h mark, followed by 500 h, 1000 h, and finally for 2000 h and above. As these are long time stretches, it is important to map experimental challenges, like electrolyte depletion, bubble blockage of the electrodes etc that can hinder the testing.

Finally, it is known that performance in rotating disc electrode (RDE) and in actual electrolysis cells can vary due to several parameters, e.g. mass transport limitations, product release from the surface etc. This is a very important aspect that will be addressed and mapped in the course of the project. Currently, the new version of Unit 1 is under construction by our partners in APRIA and as soon as this is completed both the OER and HER catalysts (the latter developed by AUTH in WP3) will be integrated in Unit 1 and be compared against the activity in the RDE experiments. In parallel, we are working on immobilizing both types of platform OER catalysts, which are in powder form, onto Ni mesh electrodes





kindly provided by the Norwegian company, NEL, which develops and supplies the market with both PEM and AEM electrolysis systems.





#### **Disclaimer**

"Funded by the European Union. Views and opinions expressed are however those of the author(s) only and do not necessarily reflect those of the European Union or the European Climate, Infrastructure and Environment Executive Agency (CINEA). Neither the European Union nor the granting authority can be held responsible for them."